The Journal of Immunology

Antigen-Specific Memory Regulatory CD4$^+$ Foxp3$^+$ T Cells Control Memory Responses to Influenza Virus Infection

Erik L. Brincks, Alan D. Roberts, Tres Cookenham, Stewart Sell, Jacob E. Kohlmeier, Marcia A. Blackman and David L. Woodland

J Immunol 2013; 190:3438-3446; Prepublished online 6 March 2013;
doi: 10.4049/jimmunol.1203140
http://www.jimmunol.org/content/190/7/3438

The Journal of Immunology is published twice each month by
The American Association of Immunologists, Inc.,
1451 Rockville Pike, Suite 650, Rockville, MD 20852

Print ISSN: 0022-1767 Online ISSN: 1550-6606.

Antigen-Specific Memory Regulatory CD4$^+$Foxp3$^+$ T Cells Control Memory Responses to Influenza Virus Infection

Erik L. Brincks,* Alan D. Roberts,* Tres Cookenham,* Stewart Sell,[†,‡] Jacob E. Kohlmeier,[§] Marcia A. Blackman,* and David L. Woodland[¶]

Regulatory CD4$^+$Foxp3$^+$ T cells (Tregs) are key regulators of inflammatory responses and control the magnitude of cellular immune responses to viral infections. However, little is known about how Tregs contribute to immune regulation during memory responses to previously encountered pathogens. In this study, we used MHC class II tetramers specific for the 311–325 peptide from influenza nucleoprotein ($NP_{311–325}/IA^b$) to track the Ag-specific Treg response to primary and secondary influenza virus infections. During secondary infections, Ag-specific memory Tregs showed accelerated accumulation in the lung-draining lymph node and lung parenchyma relative to a primary infection. Memory Tregs effectively controlled the in vitro proliferation of memory CD8$^+$ cells in an Ag-specific fashion that was MHC class II dependent. When memory Tregs were depleted before secondary infection, the magnitude of the Ag-specific memory CD8$^+$ T cell response was increased, as was pulmonary inflammation and airway cytokine/chemokine expression. Replacement of memory Tregs with naive Tregs failed to restore the regulation of the memory CD8 T cell response during secondary infection. Together, these data demonstrate the existence of a previously undescribed population of Ag-specific memory Tregs that shape the cellular immune response to secondary influenza virus challenges and offer an additional parameter to consider when determining the efficacy of vaccinations. ***The Journal of Immunology*****, 2013, 190: 3438–3446.**

Regulatory CD4$^+$Foxp3$^+$ T cells (Tregs) play important regulatory roles in the pathogenesis of cancer, autoimmune disease, and infectious disease. For example, in immune responses against tumors, Tregs dampen tumor-specific immune responses both in the local tumor microenvironment and in secondary lymphoid organs, resulting in enhanced tumor survival and metastasis (1, 2). In contrast, aberrant Treg function can be observed in a number of autoimmune diseases, including systemic lupus erythematosus, multiple sclerosis, rheumatoid arthritis, and type 1 diabetes (3, 4). During the immune response to infection, Tregs contribute to the resolution of inflammatory responses by limiting proinflammatory cytokine expression, by reducing inflammation in infected tissues, and by limiting pathogen-specific T cell responses (5–9). In many infections, Treg function is beneficial, because it limits immunopathology. However, Treg activity can also promote persistence of a pathogen, thereby turning what could be an acute/cleared infection into a chronic/persistent infection (5, 10–12). Determining the positive and negative roles Tregs play in the pathogenesis of infections is critical for the understanding of disease progression, and will also provide insights for improving the design of vaccines against specific pathogens.

A role for T regulatory cells in the control of virus infections has been implicated for a number of viruses, including respiratory syncytial virus (6, 13), HSV (9), rotavirus (14), dengue virus (15), and coronavirus (7, 16). There is increasing evidence that Tregs can be pathogen specific. For example, Treg Ag specificity has been implicated in *Toxoplasma gondii* (17) and *Leishmania major* infections (10, 18), where in vitro proliferation assays demonstrated that Tregs responded to pathogen-specific simulation. Also, after adoptive transfer of P25 TCR transgenic Tregs specific for a *Mycobacterium tuberculosis* Ag, there was Ag-specific proliferation to *Mycobacterium tuberculosis* Ags and delayed effector responses at the site of infection (11). Most recently, MHC class II tetramers specific for two epitopes expressed by the rJ2.2 strain of mouse hepatitis virus were used to identify virus-specific Tregs that were recruited during infection and contributed to regulation of effector responses (7). These data support the contribution of Ag-specific Tregs in primary infections. However, little is known about the contribution of Tregs to memory responses. Key questions are whether Ag-specific Tregs develop into a memory population and whether they play a role in regulating recall responses.

In this study, we examined memory responses to influenza virus using MHC class II tetramers to track Ag-specific CD4 T cell responses. The data indicate that Ag-specific Tregs were recruited to the lungs during secondary infection, and that the rate of recruitment was enhanced compared with a primary response. This memory Treg response influenced pulmonary inflammation and regulated Ag-specific CD8 T cell recall responses both in vitro and in vivo. The in vitro studies showed that regulation of memory CD8 T cell

*Trudeau Institute, Saranac Lake, NY 12983; [†]Division of Translational Medicine, The Wadsworth Center, New York State Department of Health, Albany, NY 12201; [‡]Department of Biomedical Sciences, School of Public Health, University at Albany, State University of New York, Albany, NY 12201; [§]Department of Microbiology and Immunology, Emory University School of Medicine, Atlanta, GA 30322; and [¶]Keystone Symposia, Silverthorne, CO 80498

Received for publication November 14, 2012. Accepted for publication February 4, 2013.

This work was supported by National Institutes of Health Grants AI076499 (to D.L.W. and M.A.B.) and T32 AI049823 (to D.L.W.), and by the Trudeau Institute.

Address correspondence and reprint requests to Dr. Marcia A. Blackman, Trudeau Institute, 154 Algonquin Avenue, Saranac Lake, NY 12983. E-mail address: mblackman@trudeauinstitute.org

The online version of this article contains supplemental material.

Abbreviations used in this article: BAL, bronchoalveolar lavage; BALT, bronchus-associated lymphoid tissue; dLN, draining lymph node; DT, diphtheria toxin; EID_{50}, 50% egg infectious dose; GITR, glucocorticoid-induced TNFR; MOI, multiplicity of infection; NP, nuclear protein; PA, acid polymerase; Penh, enhanced pause; Treg, regulatory CD4$^+$Foxp3$^+$ T cell.

www.jimmunol.org/cgi/doi/10.4049/jimmunol.1203140

proliferation required MHC class II expression on APCs and was pathogen specific. Further, adoptive transfer of naive Tregs failed to regulate the recall response of memory CD8 T cells specific for influenza virus. Together, these data support the existence of Ag-specific memory Tregs that play an important role in the regulation of immune responses to secondary infections.

Materials and Methods

Mice

C57BL/6, B6.SJL-Ptprca Pep3/BoyJ (CD45.1), and B6.PL-Thy1a/Cy (CD90.1$^+$) mice were purchased from the Trudeau Institute. Foxp3^{gfp} mice on a B6 background were provided by A. Rudensky (University of Washington, Seattle, WA). Foxp3-DTR mice on a B6 background were previously described (19) and provided by T. Sparwasser (Institute of Infection Immunology, TWINCORE, Center for Experimental and Clinical Infection Research, Hannover, Germany). Vert-X (C57BL/6 IL-10/eGFP reporter) mice were provided by M. Mohrs (Trudeau Institute). All animal studies have been reviewed and approved by the Trudeau Institute Animal Care and Usage Committee.

Viruses and infections

Influenza viruses A/HK-x31 (x31, H3N2) and A/PR8 (PR8, H1N1) were grown, stored, and titered as previously described (20). For virus infection, mice were anesthetized with 2,2,2-tribromoethanol (200 mg/kg), and virus was administered intranasally (500 50% egg infectious doses [EID_{50}] for primary PR8 infections, 300 EID_{50} for x31 infections, 5×10^4 EID_{50} for secondary PR8 infections, 3×10^5 EID_{50} for secondary x31 infections, and 250 EID_{50} for Sendai). In vitro infections were completed as described previously (21). In brief, cells were coincubated with a 10 multiplicity of infection (MOI) dose of virus for 30 min on ice, followed by 30 min at 37°C. Cells were washed two times with complete medium and cultured in 96-well plates.

Tissue harvest and flow cytometry

Mice were sacrificed at the indicated times and cells were isolated from the lung airways by bronchoalveolar lavage (BAL), the lung parenchyma by digestion in collagenase/DNase for 1 h at 37°C followed by Percoll gradient centrifugation, and the mediastinal lymph nodes and spleen by mechanical disruption. After RBC lysis with ammonium-buffered chloride, live cell numbers were determined by counting and trypan blue exclusion (20). Single-cell suspensions were incubated with Fc block (anti-CD16/32) for 15 min on ice followed by staining with influenza nuclear protein (NP), $NP_{311–325}IA^b$, $FluNP_{366–374}D^b$, Flu acid polymerase (PA), $PA_{224–233}D^b$ or Sendai $NP_{324–332}K^b$ tetramers for 1 h at room temperature. Tetramers were obtained from the National Institutes of Health Tetramer Core Facility (http://tetramer.yerkes.emory.edu) or from the Trudeau Institute Molecular Biology Core (http://www.trudeauinstitute.org). Tetramer-labeled cells were stained with Abs to CD4, CD8, CD25, CD44, CD45.1, CD45.2, CD69, CD90.1, CTLA4, glucocorticoid-induced TNF receptor (GITR) (BD Bioscience and eBioscience). For intracellular Foxp3 staining, cells were fixed, permeabilized, and stained according to Foxp3 Staining Kit protocol (eBioscience). Samples were acquired on a FACSCanto II flow cytometer (BD Biosciences), and data were analyzed with FlowJo software (Tree Star).

Assessment of cytokine production by intracellular cytokine staining

For CD8$^+$ T cell cytokine production, single-cell suspensions were incubated with $FluNP_{366–374}$ or $FluPA_{224–232}$ peptides as previously described (22). Cells were stained for surface markers, fixed, and permeabilized (CytoFix/CytoPerm kit; BD Biosciences), and stained with mAbs to IFN-γ. For CD4$^+$ T cell cytokine production, single-cell suspensions were incubated with $FluNP_{311–325}$ peptide. Cells were stained for surface markers, fixed, and permeabilized with Foxp3 Staining Kit (eBioscience), and stained with mAbs for IL-10, TGF-β, CTLA4, IFN-γ, and TNF-α (BD Biosciences, eBioscience, and R&D Systems).

Measurement of proliferation by BrdU incorporation

Measurement of proliferation by BrdU incorporation was done similarly to previously described (23). In brief, mice were administered BrdU (200 μl of a 4-mg/ml solution in PBS) i.p. and maintained on drinking water containing BrdU (0.8 mg/ml) for 24 h before harvest. Single-cell suspensions were stained with tetramers and Abs to surface proteins as described earlier, and BrdU incorporation was detected using the BrdU Flow Kit (BD Biosciences).

In vitro suppression assay

CD4$^+$ T cells were enriched by negative magnetic selection from influenza-primed *Foxp3^{gfp}* mice (pooled from 10 mice at day 35 postinfection) using a mouse CD4$^+$ T cell BD iMag enrichment kit (BD Bioscience). After enrichment of CD4$^+$ T cells, CD4$^+$GFP$^-$ and CD4$^+$GFP$^+$ T cells were then sorted using a BD FACSVantage cell sorter (BD Bioscience). For the suppression assay, $3–5 \times 10^4$ CFSE-labeled (3 μM; Invitrogen) memory CD8$^+$ T cells from influenza-infected CD90.1 mice were cocultured with varying ratios of Tregs and 10^5 CD45.1$^+$ APCs per well in a 96-well round-bottom plate. APCs had been infected with 10 MOI of influenza virus 24 h before cocultures. In some cultures, Tregs sorted from influenza-infected mice were used in cultures with memory CD8$^+$ T cells from Sendai virus–infected CD90.1 mice and APCs that had been infected in vitro with 10 MOI of Sendai virus. After 90 h, cells were harvested, stained with MHC class I tetramers, and stained for congenic surface markers and CD8. CD4$^+$ Foxp3$^-$ responder cells were analyzed for CFSE dilution by flow cytometry.

Measurement of morbidity and airway resistance

Enhanced pause (Penh) was measured using a whole-body plethysmograph similar to previously described (24) (Buxco Electronics, Sharon, CT). Penh values were recorded daily following secondary influenza virus infection. Breathing patterns were recorded for 10 mi/mouse to obtain an average Penh value. Mice were weighed daily to determine morbidity.

Measurement of airway cytokine and chemokine expression

BAL fluid was harvested from mice 5 d after secondary influenza virus challenge. Subsequently, the cytokine and chemokine expression was determined using a mouse cytokine/chemokine multiplex (Invitrogen, Carlsbad, CA).

Histological analysis

Lungs were inflated with 5 ml neutral-buffered formalin (10% v/v) via the trachea and fixed for 72 h. Lungs were embedded in paraffin wax, and 4- to 5-μm sections were mounted onto slides and stained with H&E. The inflammatory response and proliferation were assessed and scored according to scales depicted and described in Supplemental Fig. 3A and 3B by a pathologist who was blinded to the identity of the samples. All slides were viewed with an Axioplan 2 microscope, and images were captured on an Olympus BX 51 microscope equipped with fluorescence detection and Optronics PictureFrame Version 1.2 software (Center Valley, PA).

Statistical analysis

Statistical analysis was performed using Prism 5 (GraphPad Software). Significance was determined by an unpaired two-tailed Student *t* test or by two-way ANOVA with subsequent Bonferroni post hoc tests. The *p* values <0.05 were considered significant.

Results

Primary and secondary influenza virus infections induce the recruitment of Ag-specific Tregs to the lung and lung-draining lymph node

To assess the recruitment of Tregs during the primary and recall responses to influenza virus, we infected mice with H1N1 influenza virus (A/PR8, PR8) to analyze the primary infection or infected them with H3N2 influenza virus (A/HK-x31, X31) and challenged them with PR8 to analyze the recall response. At various days postinfection or challenge, the Treg (CD4$^+$Foxp3$^+$) response was quantified in the lung and lung-draining lymph node (dLN). Consistent with cellular responses to other virus infections, Tregs accumulated transiently at the site of infection, as well as in the tissue-dLN (Fig. 1). Treg recruitment to the lung-dLN was accelerated during the response to secondary challenge, and more Tregs were recruited to both the lung and the lung-dLN during responses to secondary challenge (Fig. 1A, 1E). To assess the Ag specificity of the Treg response, we stained CD4 cells with MHC class II I-A^b tetramer specific for the $FluNP_{311–324}$ epitope (Fig. 1B, 1F). Compared with naive mice, mice previously infected with influenza virus had an expanded Ag-specific Treg compartment before infection (Fig. 1B, 1F). As shown in Fig. 1C and 1G, Ag-specific Tregs accumulated in the lung and lung-dLN during both

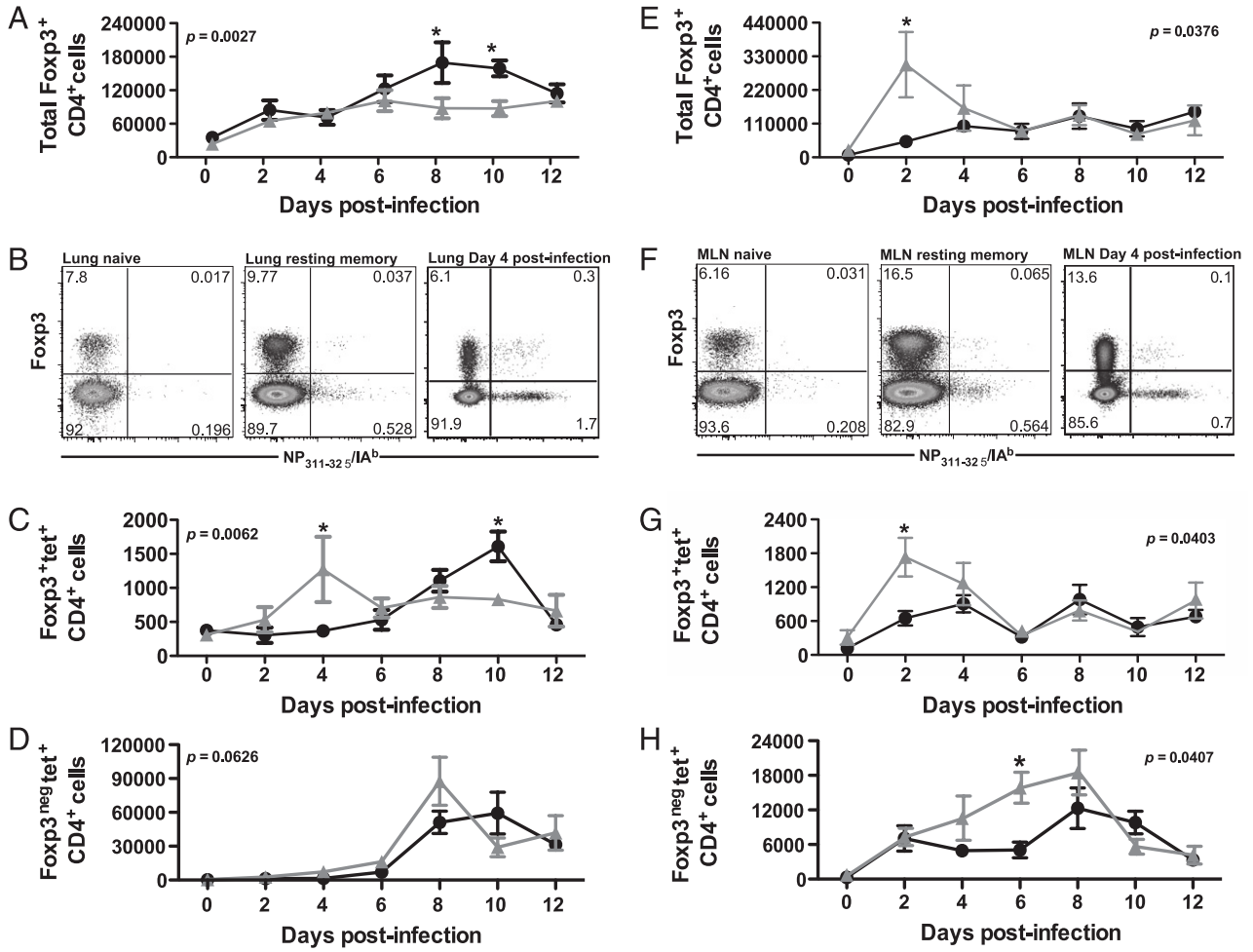

FIGURE 1. Influenza virus infection induces recruitment of Ag-specific T regulatory cells to the lung and lung-dLN. C57BL/6 mice were sacrificed at indicated times after primary (600 EID_{50} PR8 influenza virus) or secondary (60,000 EID_{50} PR8 influenza virus) infection, and lymphocytes harvested from the lung (**A**–**D**) or the lung-dLN (**E**–**H**) were stained for CD4, Foxp3, and NP_{311}/I-A^b tetramer. (A and E) Total Tregs per lung (A) or dLN (E) at various days after primary (●) or secondary (Δ) infection. (B and F) Representative plots from the lung (B) and dLN (F) gated on total $CD4^+$ cells in tissue. (C and G) Ag-specific Treg NP_{311}/I-$A^{b+}CD4^+Foxp3^+$ cells per lung (C) or dLN (G) at various days after primary (●) or secondary (Δ) infection. (D and H) Ag-specific Treg NP_{311}/I-$A^{b+}CD4^+Foxp3^{neg}$ cells per lung (D) or dLN (H) at various days after primary (●) or secondary (Δ) infection. Data are from four to five mice per time point in two independent experiments. Error bars indicate mean ± SD. (A, C–E, G, and H) Significance was determined using a two-way ANOVA. Subsequent analysis of individual time-point significance was determined by Bonferroni post hoc tests. Significance indicated as $*p < 0.05$.

primary and secondary challenge. These Ag-specific Tregs expressed molecules consistent with Treg phenotype and function, including CD25, CTLA4, and GITR (Supplemental Fig. 1). We were unable to detect IL-10 expression in the Tregs responding to secondary challenge, although IL-10 transcription was detected in Tregs during the response to primary infection (Supplemental Fig. 1). Interestingly, Ag-specific Tregs accumulated with accelerated kinetics during the response to secondary influenza virus infection relative to the response against primary infection. Also of note, the kinetics of the Ag-specific Treg response were distinct from the kinetics of Ag-specific $CD4^+Foxp3^{neg}$ cells; that is, the peak of the Ag-specific Treg response occurred earlier than the peak of the Ag-specific CD4 effector response (Fig. 1D, 1H). Consistent with previous reports of Ag-specific responses correlating with increased proliferation, the majority of Ag-specific Tregs had proliferated in response to infection (Supplemental Fig. 2). Together, these data suggest that Ag-specific Tregs are involved in the primary and recall responses to influenza virus infection, and the accelerated recruitment during recall responses suggests the existence of a population of Ag-specific memory Tregs that persists in the host.

Memory Tregs regulate in vivo inflammation during the recall response to influenza virus infection

The pulmonary immune response to secondary influenza infections involves not only an Ag-specific T cell response, but also an inflammatory response characterized by chemokine and cytokine production, as well as alterations to the pulmonary architecture. To assess the role of memory Tregs in regulating pulmonary inflammation, we infected mice with x31 and challenged them with PR8, with or without anti-CD25 mAb treatment before challenge. This treatment resulted in a depletion of 70–80% of the existing $Foxp3^+CD4^+$ Tregs (data not shown). Scoring of histology sections revealed increased inflammation and epithelial proliferation in the mice that had been depleted of Tregs (Fig. 2A, 2B). Grading of inflammation is based on both the nature of the lesion and the degree of involvement (Supplemental Fig. 3A). Inflammation consists of a mixed mononuclear cell infiltrate that varies from small compact foci through large, dense areas, (Supplemental Fig. 3A). Similar dense areas of lymphoid tissue have been seen in chronic lung infections in humans and have been identified as bronchus-associated lymphoid tissue (BALT) (25). BALT is also

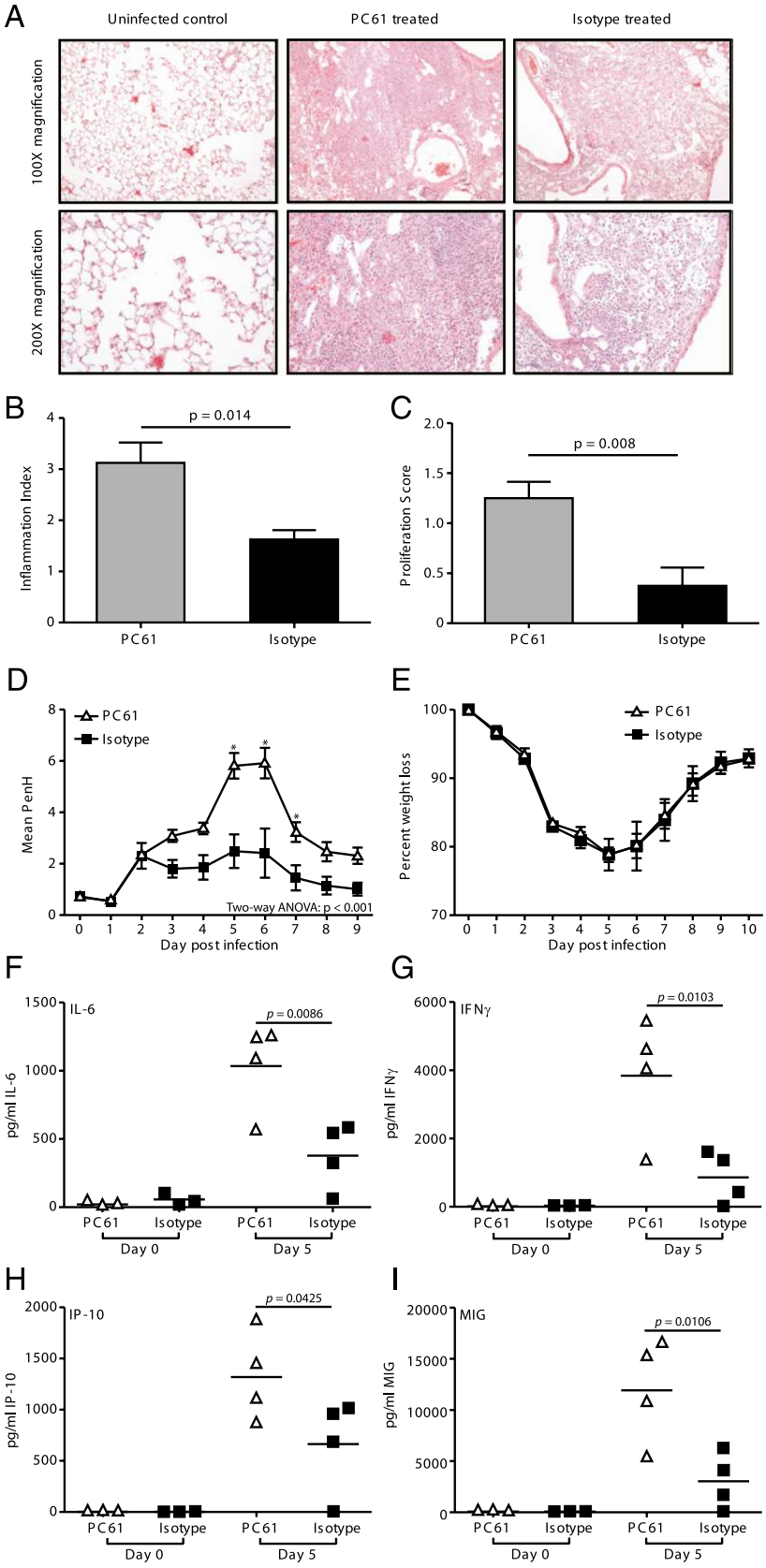

FIGURE 2. Depletion of Treg populations during influenza virus infection results in increased pulmonary inflammation. C57BL/6 mice were infected with 3000 EID_{50} x31 influenza virus and allowed to rest for 35 d. Mice were treated with PC61 or isotype control, then challenged with 60,000 EID_{50} PR8 influenza virus. On day 5 postinfection, whole lungs were harvested, fixed, sectioned, and H&E stained. (**A**) Representative lung tissue sections of uninfected lungs; lungs from infected, PC61-treated mice; or lungs from infected isotype-treated mice. (**B** and **C**) Lung sections were scored for inflammation (B) and proliferation (C). Data are representative of two independent experiments that included four mice per group. Error bars indicate mean ± SD. Differences between the histology scoring data were determined by the Mann–Whitney *U* nonparametric test. (**D**) A whole-body plethysmograph was used to measure airway resistance on a daily basis after challenge. The baseline Penh is shown as mean ± SD. Data shown are representative of two independent experiments that included four mice per group. (**E**) Weight loss was used as a measure of morbidity on a daily basis after challenge. Data show body weight as a percentage of weight at time of infection. Data are representative of two independent experiments and include four to five mice per group. (**F–I**) BAL fluid was harvested and analyzed for the proinflammatory cytokines IL-6 (F) and IFN-γ (G) and chemokines IFN-γ–inducible protein 10 (IP-10) (H) and monokine induced by IFN-γ (MIG) (I). (B, C, F–I) Differences between groups were determined by Student *t* test. (D and E) Significance was determined using a two-way ANOVA. Subsequent analysis of individual time-point significance was determined by Bonferroni post hoc tests. Significance indicated as $*p < 0.05$.

seen in mice with repeated virus infections of the lung (26). The conversion of areas of the lung next to bronchi into BALT is much greater in mice depleted of Tregs than in mice with Tregs, which feature loose collections of large monocytes with retention of alveolar structure.

Even more impressive are large areas in which the alveolar spaces were filled with epithelial cells (Supplemental Fig. 3B). As indicated by the proliferation score, proliferation of type II pneumocytes was much greater in mice depleted of Tregs (Fig. 2A, 2C). It is well documented that such proliferation is seen in mice

infected with flu virus beginning with 3–6 d post primary infection (27) and peaking in the alveoli at ~2 wk (27–29). As stated by Straub in 1937 (30): "A chronic reparative process in surviving mice has, indeed, been regularly met with. This is not, as so often in man, fibrous but epithelial in nature. The epithelium of the terminal bronchioles proliferates and becomes more or less stratified.…The proliferation does not stop here, but regularly invades the lung tissue. It first enters the respiratory bronchioles and next the alveoli." In the absence of Tregs, this exaggerated repair response expands to occupy >50% of the lung tissue on histologic slides. Squamous metaplasia was not seen, most likely because it was only 5 d post secondary infection.

Treg depletion did not alter morbidity (Fig. 2E), mortality, or virus clearance, but did result in increased Penh compared with the isotype-treated mice (Fig. 2D), suggesting that the lungs of depleted mice had increased pathology and decreased lung function. Consistent with the H&E scoring and the Penh evaluations, mice depleted of Tregs had increased pulmonary chemokine (IFN-γ–inducible protein 10 and monokine induced by IFN-γ) and cytokine (IL-6 and IFN-γ) expression compared with isotype control-treated mice (Fig. 2F–I). Together, these data suggest that memory Tregs contribute to the control of pulmonary inflammation during the recall response to secondary challenge.

Memory Tregs regulate the in vivo memory CD8 T cell response to influenza virus infection

To complement the studies of pulmonary inflammation induced by influenza virus infection, we investigated the role of memory Tregs in controlling secondary influenza infection. Mice were infected with x31 and challenged 35 d later with PR8, with anti-CD25 mAb (PC61) or isotype control Ab for 2 d before challenge. Five days post-PR8 challenge, the influenza-specific CD8 T cell response was measured using MHC class I tetramers specific for two immunodominant influenza virus epitopes, nucleoprotein ($NP_{366–374}/D^b$) and acid polymerase ($PA_{224–233}/D^b$; Fig. 3A). Depletion of Tregs increased the magnitude of the pulmonary tetramer-specific CD8 T cell response (Fig. 3B, 3C), and more of these CD8 T cells produced IFN-γ during the recall response (Fig. 3D, 3E). These data support a role for memory Tregs in controlling the in vivo memory CD8 T cell response to secondary influenza virus infection.

The functional regulation of memory responses suggests that memory Tregs are maintained after a primary infection. However, an alternative explanation is that memory CD8 T cells are more susceptible to regulation by Tregs than naive T cells. That is, memory CD8 T cell responses to secondary infection could be similarly regulated by any Treg population responding to infection, be they Ag-inexperienced Tregs or memory Tregs. To compare the function of memory Tregs and naive Tregs in regulating a memory CD8 T cell response, we used the Foxp3-DTR mice, in which cells expressing Foxp3 also express the diphtheria toxin (DT) receptor on their cell surface. Foxp3-DTR mice previously infected with influenza virus were treated with DT before secondary infection to deplete memory Tregs (Fig. 4A). DT treatment depleted both $tetramer^+$ and $tetramer^-$ $Foxp3^+$ cells whereas leaving the Ag-specific $CD4^+Foxp3^{neg}$ cells intact in both the lung and the lung-dLN (Fig. 4B, 4C). Similar to the results observed using PC61 mAb treatment to deplete memory Tregs, the depletion of Tregs by DT resulted in an increased Ag-specific CD8 T cell response at day 5 postinfection (Fig. 4D, 4E). In contrast, the adoptive transfer of naive Tregs (to replace the depleted memory Tregs; Fig. 4B, 4C) resulted in CD8 T cell responses similar to those in mice that had no Tregs (Fig. 4D, 4E). Only in mice in which the memory Treg population had not been depleted was the Ag-specific CD8 T cell response to secondary infection reduced. This regulatory function, together with the accelerated recruitment kinetics observed in Fig. 1, suggests that influenza virus infection results in the formation of a pool of memory Tregs with the capacity to regulate immune responses to subsequent challenge with virus in an Ag-specific fashion. Considered together, the Ab depletion and DT depletion data suggest that Ag-specific memory Tregs, and not naive Tregs, are important players in the control of pulmonary inflammation and the regulation of memory CD8 T cell responses.

Memory Tregs regulate proliferation of memory CD8 T cells in an Ag-specific fashion that requires MHC class II

A defining characteristic of T regulatory cells is their ability to regulate immune responses, including their ability to inhibit the proliferation of CD8 T cells that have been stimulated through their TCR with anti-CD3 or with Ag. To complement in vivo studies of the influenza-specific memory Treg function, we isolated memory Tregs from influenza-infected mice and used them to inhibit the proliferation of memory CD8 T cells stimulated in vitro by co-culture with infected APCs (see Supplemental Fig. 4 for outline of experimental design, cell sources, and culture combinations). When the cultures contained only memory CD8 T cells and APC, significant CD8 T cell proliferation was observed. When memory $CD4^+Foxp3^+$ Tregs, but not memory $CD4^+Foxp3^{neg}$ cells, were added to the CD8/APC cocultures, proliferation of the memory CD8 T cells was significantly decreased (Fig. 5A, 5B). Increasing the ratio of $FluNP_{366}$-specific CD8 memory cells to influenza-specific Tregs (culture + Treg in Fig. 5C) resulted in the decrease and eventual loss of inhibitory effect of the memory Tregs. In contrast, altering the ratio of NP_{366}-specific CD8 memory cells to influenza-specific $CD4^+Foxp3^{neg}$ cells (culture + CD4 in Fig. 5C) in the cultures did not influence the proliferation of the CD8 effectors.

To assess the pathogen specificity of the inhibitory function of the memory Tregs, influenza-specific Tregs were used to inhibit proliferation of Sendai virus NP_{324}-specific memory CD8 cells that had been stimulated by Sendai virus-infected APCs. The populations of influenza-specific memory Tregs and memory CD4 effectors (i.e., those that were used in Fig. 5A–C) were used to inhibit the proliferation of Sendai virus NP_{324}-specific CD8 effectors. Neither the addition of influenza-specific memory Tregs nor the addition of influenza-specific CD4 effectors influenced the proliferation by the Sendai virus NP_{324}-specific CD8 T cells (Fig. 5D). Furthermore, altering the ratio of CD8 effectors to Tregs did not influence the proliferation. Together with the data from Fig. 5C, these data support a model in which the inhibitory function by memory Tregs requires recognition of cognate Ag.

CD8/APC/Treg cultures were set up using APC from MHC class II–deficient mice to investigate the requirement for MHC class II in Treg function. In the absence of MHC class II on the influenza-infected APCs to present Ags to CD4 cells, there was no inhibition of CD8 proliferation by the influenza-specific memory Tregs (Fig. 5E). Of note, Tregs harvested from infected lungs, from the lung-dLN, or from the spleen all had similar capacity to inhibit memory CD8 T cell proliferation (Fig. 5E). Together, these data demonstrate that influenza-specific memory Tregs regulate the recall response of memory CD8 T cells in a pathogen-specific, MHC class II–dependent manner.

Discussion

There are two possible models for Treg control of CD8 T cell function: an indirect two-step model involving APCs or a direct model. The requirement for MHC class II expression on APCs supports the possibility that interactions between memory Tregs and APCs could lead to deactivation of the APC. These interactions

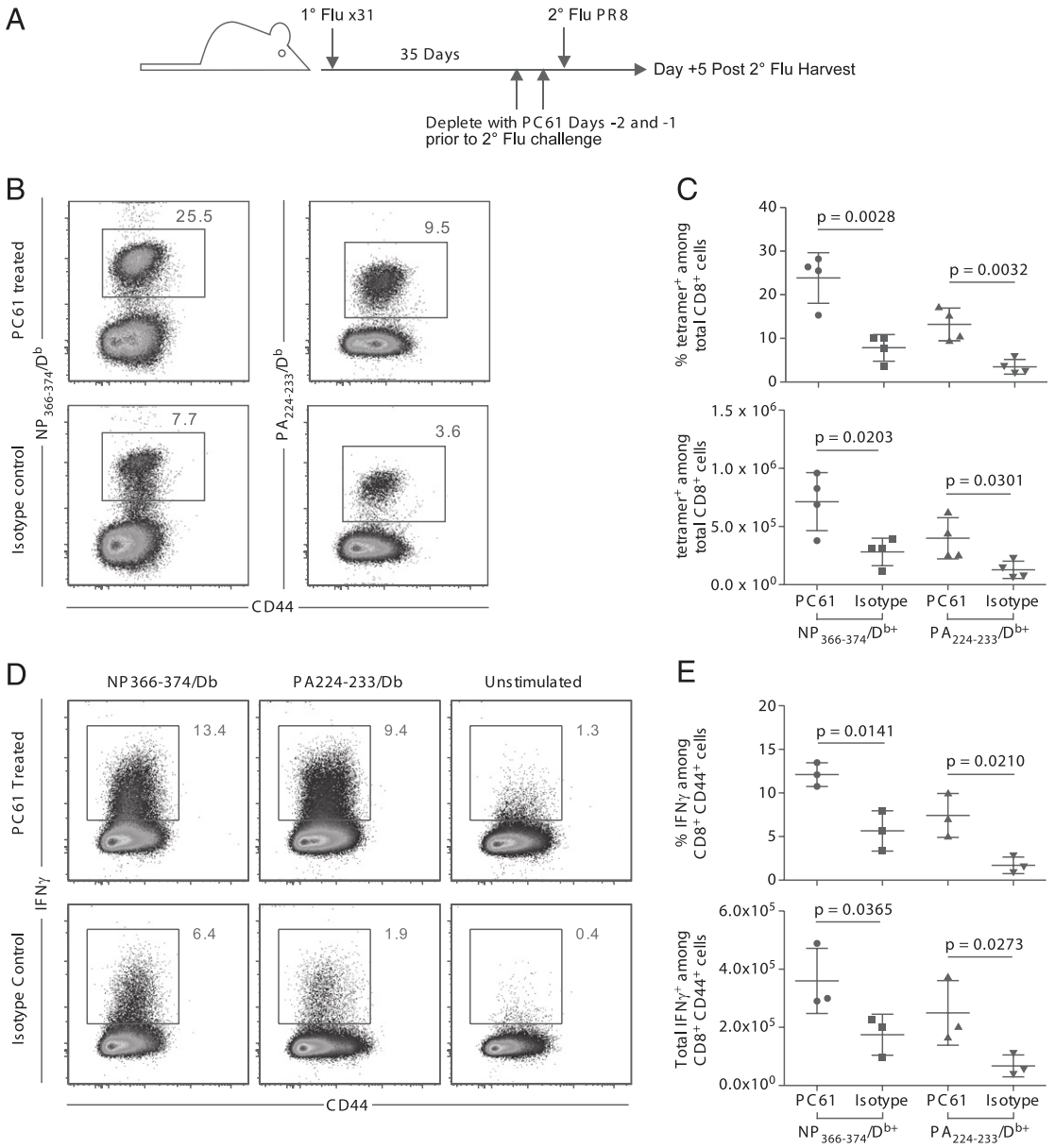

FIGURE 3. Memory Tregs regulate the magnitude of in vivo influenza-specific CD8 T cell responses to secondary challenge. C57BL/6 mice were infected with 3000 EID_{50} x31 influenza virus and allowed to rest for 35 d. Mice were treated with PC61 or isotype control, then challenged with 60,000 EID_{50} PR8 influenza virus and sacrificed at day 5 postinfection. (**A**) Schematic of experimental design that outlines infections, Ab treatments, and harvests. (**B** and **C**) Lymphocytes were isolated from the lungs and stained with FluNP_{366}/D^b tetramer or PA_{224}/D^b tetramer. (B) Representative staining of influenza-specific CD8 T cell responses in the lung. Plots are gated on $CD8^+$ cells. (C) Percentage of $tetramer^+$ cells among total $CD8^+$ cells in the lung (*top panel*) and total $tetramer^+$ cells per lung (*bottom panel*). (**D** and **E**) Lymphocytes were isolated from the lungs and analyzed for IFN-γ production after peptide stimulation. (D) Representative plots for IFN-γ production by $CD8^+$ T cells after stimulation with NP_{366} peptide-pulsed, PA_{224} peptide-pulsed, or unpulsed APCs. (E) Percentage of IFN-γ^+ cells among total $CD8^+$ cells in the lung (*top panel*). Total IFN-γ^+ cells per lung (*bottom panel*). Data points represent individual mice. Lines represent mean. Error bars represent SD. Data are representative of three independent experiments. Differences between groups were determined by Student *t* tests.

could take place in the lung-dLN or in the infected lung environment, because recall responses include activation of T cells in both. Such a model would be consistent with reports that Treg–DC interactions can alter subsequent immune responses (31, 32). Alternatively, memory Tregs might interact directly with memory CD8 T cells to inhibit their proliferation (33, 34).

In a two-step model of Treg function, memory Tregs would interact with APC-expressing influenza Ags, thereby activating the Tregs. Subsequently, the activated memory Tregs, or soluble factors secreted by these Tregs, would interact with the CD8 T cells, thereby blocking their proliferation. During the recall response, the Ag-specific Tregs expressed surface markers consistent with regulatory function (35) (e.g., CD25, CTLA4, GITR), but we were unable to detect the production of IL-10, IFN-γ, TGF-β, or TNF-α in these cells after stimulation with Ag. The lack of cytokine production suggests that their regulatory function is via a cell-contact–dependent mechanism. Although the specific mechanisms of regulation have not been explicitly determined, prior studies of Treg regulatory mechanisms suggest that multiple mechanisms likely contribute to the regulation (e.g., CTLA4, TRAIL) (35, 36).

Measuring Treg function commonly involves using Tregs to block proliferation of CD8 stimulated with anti-CD3/anti-CD28 stimulation or with PMA/ionomycin stimulation of the cells in

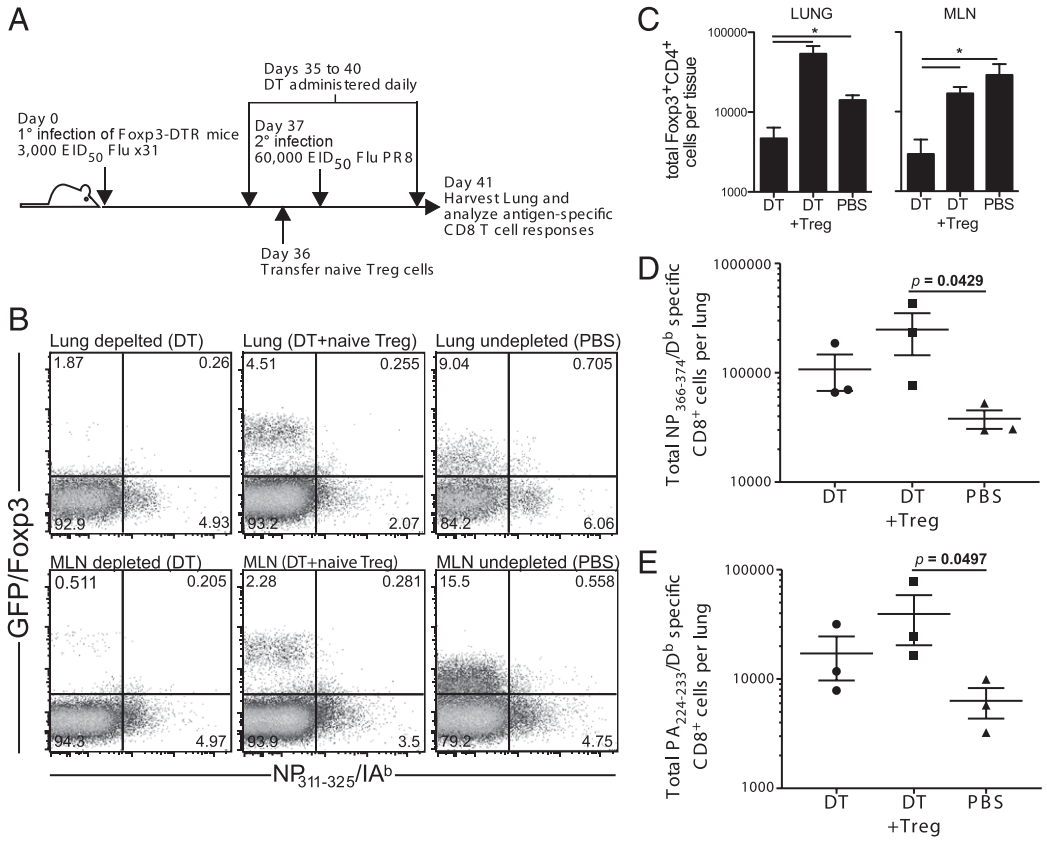

FIGURE 4. Memory Tregs are required to regulate the magnitude of in vivo influenza-specific CD8 T cell responses to secondary challenge. Foxp3-DTR mice were infected with 3000 EID_{50} x31 influenza virus and allowed to rest for 35 d. Mice were treated with DT or vehicle, then challenged with 60,000 EID_{50} PR8 influenza virus. In some mice, naive Tregs were adoptively transferred before infection. Mice were sacrificed at day 5 postinfection. Lymphocytes were isolated from the lungs and stained with $FluNP_{366}/D^b$ tetramer or PA_{224}/D^b tetramer. (**A**) Schematic of experimental design that outlines infections, DT treatments, adoptive transfer, and harvest. (**B**) Representative plots from the lung (*top row*) and dLN (*bottom row*) gated on total $CD4^+$ cells in tissue harvested from mice treated with DT, treated with DT with a transfer of naive Tregs (DT + Treg), or untreated (PBS). (**C**) Total $Foxp3^+CD4^+$ cells per tissue for both the lung (*left panel*) and the lung-dLN (*right panel*). (**D**) Total $FluNP_{366}/D^b$ $tetramer^+$ cells among total $CD8^+$ cells in the lung. (**E**) Total $FluPA_{224}/D^b$ $tetramer^+$ cells among total $CD8^+$ cells in the lung. Data points in (D) and (E) represent individual mice. Lines represent mean. Error bars represent SD. Data are representative of two independent experiments of three to four mice per group. Differences between groups were determined by Student *t* tests. Significance indicated as $*p < 0.05$.

culture (7, 9, 10). Contrary to previous investigations of infection, this study used a more physiological approach in which Tregs were used to block memory CD8 T cell proliferation that was stimulated by influenza-infected APCs. Using this pathogen-specific assay, we found that memory Tregs from an influenza-primed host effectively suppressed the proliferation of influenza-specific memory CD8 T cells stimulated with influenza-infected APCs. However, when those same influenza-specific Tregs were placed into cultures with Sendai virus–infected APCs presenting to Sendai-specific CD8 memory cells, the Tregs failed to block proliferation, suggesting that the regulatory functions of Tregs are pathogen specific. Further, Treg function also appears to require TCR stimulation, because the absence of MHC class II expression on the influenza-infected APCs resulted in minimal regulation of CD8 proliferation by the memory Tregs. These data suggest that Tregs require TCR stimulation for optimal activity, and that the regulatory functions of Tregs might be more restricted than previously suggested by data from cultures using anti-CD3/anti-CD28 stimulation of CD8 T cells. In those experiments, the Abs used to trigger CD8 effector proliferation would also stimulate Treg activation in a nonspecific fashion. Future studies should take this potential complicating factor into consideration and more specifically examine the requirement for Ag-specific Treg activation when assessing Treg function in vitro.

Our findings have substantial implications for vaccination strategies, as we were also able to find Ag-specific memory Treg populations after whole-protein vaccination with FluNP (data not shown). Eliciting an Ag-specific Treg response could be beneficial during influenza virus infections, as well as other infections where immunopathology is a concern, including coronavirus (7, 16), dengue virus (15), and respiratory syncytial virus (6, 13). Vaccination attempts to limit pathology in autoimmune disease could aim to elicit Ag-specific Treg responses, although identifying target Ags would be an obvious obstacle in the context of autoimmunity (3, 4). In the context of tumor immunology, the activation of Tregs during protein vaccinations against tumor Ags would be a serious concern, because multiple tumor models have demonstrated that Tregs limit the efficacy of immunotherapy efforts (1, 2). Clearly, future studies of vaccination strategies need to consider potential vaccine-specific Treg responses and how such responses might influence the desired effect of the vaccine.

Taken together, our findings suggest a previously unappreciated population of Ag-specific memory Tregs that regulate immune responses during secondary encounters with pathogens. Although Tregs have been recognized as cells that are constitutively activated and can rapidly respond to inflammation, we propose that the requirement of Ag recognition provides a critical checkpoint to

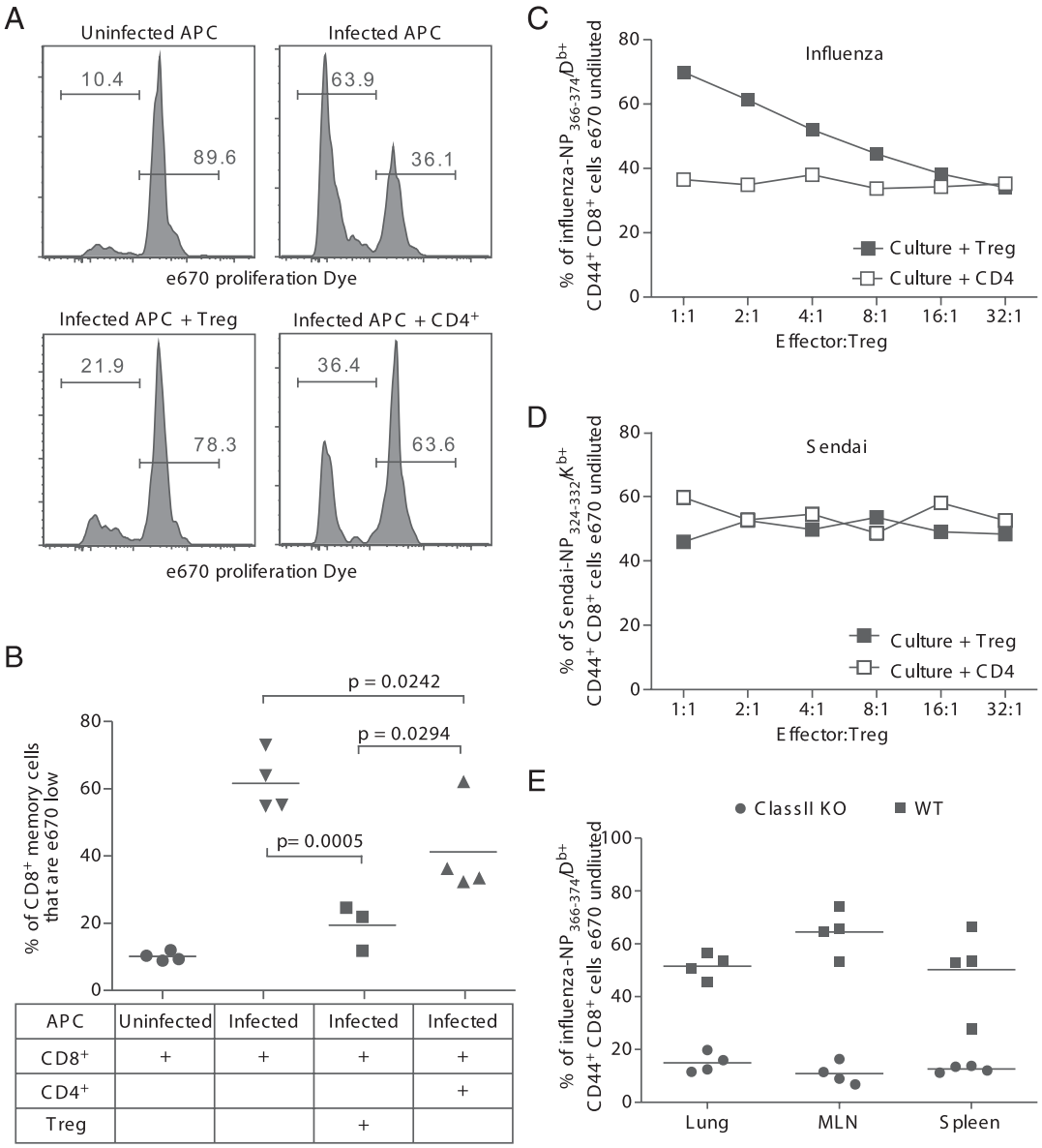

FIGURE 5. Tregs responding to influenza virus challenge inhibit memory T cell proliferation in an Ag-specific fashion. Foxp3-GFP mice were infected with 3000 EID_{50} x31 influenza virus and allowed to rest for 35 d. Mice were then challenged with 60,000 EID_{50} PR8 influenza virus and sacrificed at day 4 postinfection. Lymphocytes were isolated from the lungs, dLN, and spleen, enriched for $CD4^+$ cells, and sorted into GFP^+ (Treg) and GFP^- (CD4 effector) populations, and used to inhibit the proliferation of influenza-specific CD8 T cells stimulated with influenza-infected APCs. (**A**) Representative histograms demonstrating the inhibition of CD8 T cell proliferation when Tregs are added to wells. Histogram plots are gated on congenic $marker^+CD8^+$ cells. (**B**) The frequency of total $CD8^+$ effector cells that had proliferated after coculture with influenza-infected APCs. Data points represent individual wells; bar represents mean. Data in (A) and (B) are representative of two independent experiments, in which cells were pooled from 12–15 Foxp3-GFP mice for each experiment. (**C** and **D**) To assess proliferation of Ag-specific CD8 T cells, we used influenza-specific Tregs to suppress proliferation of either influenza-specific CD8 T cells (C) or Sendai virus–specific CD8 T cells (D). To identify Ag-specific effector T cells, we stained cells from proliferation assays with $FluNP_{366}/D^b$ tetramer (C) or Sendai $NP_{324}K^b$ tetramer (D). The frequency of tet^+CD8^+ that had not proliferated is displayed for each ratio of CD8:Treg (■) or CD8:CD4 (□). Data from (C) and (D) are concatenated from four to five wells for each ratio. Data in (C) and (D) are representative of 3 independent experiments, in which cells were pooled from 12–15 Foxp3-GFP mice for each experiment. (**E**) To assess the requirement of MHC class II for Treg function, we used influenza-specific Tregs from lung, dLN, or spleen to suppress proliferation of influenza-specific CD8 T cells in cultures with influenza-infected WT (■) or class II knockout (●) APCs. Cells from proliferation assays were stained with $FluNP_{366}/D^b$ tetramer. The frequency of tet^+CD8^+ that had not proliferated is displayed for each tissue. Data points represent individual wells; bar represents mean. Data in (E) are representative of three independent experiments, in which cells were pooled from 12–15 Foxp3-GFP mice for each experiment.

Treg activation and subsequent regulatory function. During secondary infection, Treg suppression of immune responses is not global; rather, Treg activation is specific to the pathogen and results in regulation of pathogen-specific responses. Thus, secondary infection with a pathogen stimulates a memory T cell response that rapidly and vigorously controls the pathogen whereas concomitantly stimulating a memory Treg response that rapidly and vigorously controls the immune response and limits immunopathology.

Acknowledgments

We thank the Trudeau Institute Molecular Biology Core for the production of MHC class I and II tetramers, the National Institutes of Health Tetramer

Core Facility for the production of MHC class II tetramers, Mike Tighe of the Trudeau Institute imaging core for sectioning and microscopy assistance, and Brandon Sells and Ron Lacourse of the Trudeau Institute flow cytometry core for cell sorting.

Disclosures

The authors have no financial conflicts of interest.

References

1. Côté, A. L., E. J. Usherwood, and M. J. Turk. 2008. Tumor-specific T-cell memory: clearing the regulatory T-cell hurdle. *Cancer Res.* 68: 1614–1617.
2. Curiel, T. J. 2007. Tregs and rethinking cancer immunotherapy. *J. Clin. Invest.* 117: 1167–1174.
3. Buckner, J. H. 2010. Mechanisms of impaired regulation by CD4(+)CD25(+)FOXP3 (+) regulatory T cells in human autoimmune diseases. *Nat. Rev. Immunol.* 10: 849–859.
4. Long, S. A., and J. H. Buckner. 2011. CD4+FOXP3+ T regulatory cells in human autoimmunity: more than a numbers game. *J. Immunol.* 187: 2061–2066.
5. Belkaid, Y., and B. T. Rouse. 2005. Natural regulatory T cells in infectious disease. *Nat. Immunol.* 6: 353–360.
6. Fulton, R. B., D. K. Meyerholz, and S. M. Varga. 2010. Foxp3+ CD4 regulatory T cells limit pulmonary immunopathology by modulating the CD8 T cell response during respiratory syncytial virus infection. *J. Immunol.* 185: 2382–2392.
7. Zhao, J., J. Zhao, C. Fett, K. Trandem, E. Fleming, and S. Perlman. 2011. IFN-γ- and IL-10-expressing virus epitope-specific Foxp3(+) T reg cells in the central nervous system during encephalomyelitis. *J. Exp. Med.* 208: 1571–1577.
8. Suvas, S., A. K. Azkur, B. S. Kim, U. Kumaraguru, and B. T. Rouse. 2004. CD4+ CD25+ regulatory T cells control the severity of viral immunoinflammatory lesions. *J. Immunol.* 172: 4123–4132.
9. Suvas, S., U. Kumaraguru, C. D. Pack, S. Lee, and B. T. Rouse. 2003. CD4+ CD25+ T cells regulate virus-specific primary and memory CD8+ T cell responses. *J. Exp. Med.* 198: 889–901.
10. Belkaid, Y., C. A. Piccirillo, S. Mendez, E. M. Shevach, and D. L. Sacks. 2002. CD4+CD25+ regulatory T cells control *Leishmania major* persistence and immunity. *Nature* 420: 502–507.
11. Shafiani, S., G. Tucker-Heard, A. Kariyone, K. Takatsu, and K. B. Urdahl. 2010. Pathogen-specific regulatory T cells delay the arrival of effector T cells in the lung during early tuberculosis. *J. Exp. Med.* 207: 1409–1420.
12. Suvas, S., and B. T. Rouse. 2006. Treg control of antimicrobial T cell responses. *Curr. Opin. Immunol.* 18: 344–348.
13. Lee, D. C., J. A. Harker, J. S. Tregoning, S. F. Atabani, C. Johansson, J. Schwarze, and P. J. Openshaw. 2010. CD25+ natural regulatory T cells are critical in limiting innate and adaptive immunity and resolving disease following respiratory syncytial virus infection. *J. Virol.* 84: 8790–8798.
14. Kim, B., N. Feng, C. F. Narváez, X. S. He, S. K. Eo, C. W. Lim, and H. B. Greenberg. 2008. The influence of CD4+ CD25+ Foxp3+ regulatory T cells on the immune response to rotavirus infection. *Vaccine* 26: 5601–5611.
15. Dejnirattisai, W., T. Duangchinda, C. L. Lin, S. Vasanawathana, M. Jones, M. Jacobs, P. Malasit, X. N. Xu, G. Screaton, and J. Mongkolsapaya. 2008. A complex interplay among virus, dendritic cells, T cells, and cytokines in dengue virus infections. *J. Immunol.* 181: 5865–5874.
16. Trandem, K., D. Anghelina, J. Zhao, and S. Perlman. 2010. Regulatory T cells inhibit T cell proliferation and decrease demyelination in mice chronically infected with a coronavirus. *J. Immunol.* 184: 4391–4400.
17. Oldenhove, G., N. Bouladoux, E. A. Wohlfert, J. A. Hall, D. Chou, L. Dos Santos, S. O'Brien, R. Blank, E. Lamb, S. Natarajan, et al. 2009. Decrease of Foxp3+ Treg cell number and acquisition of effector cell phenotype during lethal infection. *Immunity* 31: 772–786.
18. Suffia, I. J., S. K. Reckling, C. A. Piccirillo, R. S. Goldszmid, and Y. Belkaid. 2006. Infected site-restricted Foxp3+ natural regulatory T cells are specific for microbial antigens. *J. Exp. Med.* 203: 777–788.
19. Lahl, K., C. Loddenkemper, C. Drouin, J. Freyer, J. Arnason, G. Eberl, A. Hamann, H. Wagner, J. Huehn, and T. Sparwasser. 2007. Selective depletion of Foxp3+ regulatory T cells induces a scurfy-like disease. *J. Exp. Med.* 204: 57–63.
20. Kohlmeier, J. E., W. W. Reiley, G. Perona-Wright, M. L. Freeman, E. J. Yager, L. M. Connor, E. L. Brincks, T. Cookenham, A. D. Roberts, C. E. Burkum, et al. 2011. Inflammatory chemokine receptors regulate CD8(+) T cell contraction and memory generation following infection. *J. Exp. Med.* 208: 1621–1634.
21. Brincks, E. L., T. A. Kucaba, K. L. Legge, and T. S. Griffith. 2008. Influenza-induced expression of functional tumor necrosis factor-related apoptosis-inducing ligand on human peripheral blood mononuclear cells. *Hum. Immunol.* 69: 634–646.
22. Brincks, E. L., A. Katewa, T. A. Kucaba, T. S. Griffith, and K. L. Legge. 2008. CD8 T cells utilize TRAIL to control influenza virus infection. *J. Immunol.* 181: 4918–4925.
23. Kohlmeier, J. E., L. M. Connor, A. D. Roberts, T. Cookenham, K. Martin, and D. L. Woodland. 2010. Nonmalignant clonal expansions of memory CD8+ T cells that arise with age vary in their capacity to mount recall responses to infection. *J. Immunol.* 185: 3456–3462.
24. Brincks, E. L., P. Gurung, R. A. Langlois, E. A. Hemann, K. L. Legge, and T. S. Griffith. 2011. The magnitude of the T cell response to a clinically significant dose of influenza virus is regulated by TRAIL. *J. Immunol.* 187: 4581–4588.
25. Tschernig, T., and R. Pabst. 2000. Bronchus-associated lymphoid tissue (BALT) is not present in the normal adult lung but in different diseases. *Pathobiology* 68: 1–8.
26. Chen, H. D., A. E. Fraire, I. Joris, R. M. Welsh, and L. K. Selin. 2003. Specific history of heterologous virus infections determines anti-viral immunity and immunopathology in the lung. *Am. J. Pathol.* 163: 1341–1355.
27. Nelson, A. A., and J. W. Oliphant. 1939. Histopathological changes in mice inoculated with influenza virus. *Public Health Reports (1896-1970)* 2044–2054.
28. Dubin, I. N. 1945. A pathological study of mice infected with the virus of swine influenza. *Am. J. Pathol.* 21: 1121–1141.
29. Loosli, C. G. 1949. The pathogenesis and pathology of experimental air-borne influenza virus A infections in mice. *J. Infect. Dis.* 84: 153–168.
30. Straub, M. J. 1937. The microscopial changes in the lungs of mice infected with influenza virus. *Pathology* 45: 75–78.
31. Mahnke, K., T. Bedke, and A. H. Enk. 2007. Regulatory conversation between antigen presenting cells and regulatory T cells enhance immune suppression. *Cell. Immunol.* 250: 1–13.
32. Tang, Q., J. Y. Adams, A. J. Tooley, M. Bi, B. T. Fife, P. Serra, P. Santamaria, R. M. Locksley, M. F. Krummel, and J. A. Bluestone. 2006. Visualizing regulatory T cell control of autoimmune responses in nonobese diabetic mice. *Nat. Immunol.* 7: 83–92.
33. Chen, M. L., M. J. Pittet, L. Gorelik, R. A. Flavell, R. Weissleder, H. von Boehmer, and K. Khazaie. 2005. Regulatory T cells suppress tumor-specific CD8 T cell cytotoxicity through TGF-beta signals in vivo. *Proc. Natl. Acad. Sci. USA* 102: 419–424.
34. May, K. F., Jr., X. Chang, H. Zhang, K. D. Lute, P. Zhou, E. Kocak, P. Zheng, and Y. Liu. 2007. B7-deficient autoreactive T cells are highly susceptible to suppression by CD4(+)CD25(+) regulatory T cells. *J. Immunol.* 178: 1542–1552.
35. Vignali, D. A., L. W. Collison, and C. J. Workman. 2008. How regulatory T cells work. *Nat. Rev. Immunol.* 8: 523–532.
36. Pillai, M. R., L. W. Collison, X. Wang, D. Finkelstein, J. E. Rehg, K. Boyd, A. L. Szymczak-Workman, T. Doggett, T. S. Griffith, T. A. Ferguson, and D. A. Vignali. 2011. The plasticity of regulatory T cell function. *J. Immunol.* 187: 4987–4997.